Influence of Normal and Inverse Upconversion Processes on the Continuous Wave Operation of the Er^{3+} 3 μm Crystal Laser

M. Pollnau, W. Lüthy, and H. P. Weber
Institute of Applied Physics, University of Bern, Sidlerstr. 5, CH-3012 Bern, Switzerland

Abstract

A computer simulation of the dynamics of the Er^{3+} 3 μm cw crystal laser considering the full rate-equation scheme up to the $^4F_{7/2}$ level has been performed. The influence of the important system parameters on lasing and the interaction of these parameters has been clarified with multiple-parameter variations.

Stimulated emission is fed mainly by up-conversion from the lower laser level and in many cases is reduced by the quenching of the lifetime of this level. However, also without upconversion a set of parameters can be found that allows lasing.

For a typical experimental situation we started with the parameters of Er^{3+}:$LiYF_4$. In addition also the host materials YAG, $YAlO_3$, YSGG, and BaY_2F_8 as well as the possibilities of co-doping are discussed.

Introduction

In recent years there has been enormous theoretical and practical interest in the Er^{3+} 3 μm laser. Its possible application in surgery evoked large efforts to increase the power and efficiency of the laser and to reduce its size [1-6]. Several attempts have been made [1-9] to understand cw operation on a transition which is believed to be self-terminating due to the longer lifetime of the lower laser level.

Possible reasons for the nevertheless occurance of cw lasing proposed so far include 1) depletion of the lower laser level $^4I_{13/2}$ due to excited-state absorption, 2) cross relaxation from the $^4S_{3/2}$ level and a subsequent fast multiphonon decay into the upper laser level $^4I_{11/2}$, 3) upconversion from the $^4I_{13/2}$ level feeding the $^4I_{11/2}$ level, and 4) a relatively long lifetime of the $^4I_{11/2}$ level in combination with a low braching ratio from the $^4I_{11/2}$ level into the $^4I_{13/2}$ level. All these explanations, however, consider only a single aspect and cannot describe a complex system like Er^{3+}.

In our paper we present a computer simulation of the Er^{3+} 3 μm laser, which includes, to our knowledge for the first time, all excited levels up to $^4F_{7/2}$, all lifetimes and branching ratios, ground-state depletion, excited-state absorption, three upconversion processes as well as their inverse processes, stimulated emission, and a real resonator design. Especially the inclusion of the inverse upconversion processes gives deeper insight into the population mechanisms of the system.

Computer Simulation

The standard parameters of our rate-equation model closely match the case of Er^{3+}:$LiYF_4$. The labelling of the levels is indicated in Fig. 1. The $^2H_{11/2}$ level is thermally coupled with the $^4S_{3/2}$ level.

The intrinsic lifetimes of the levels are taken as: τ_1 = 10 ms, τ_2 = 4.8 ms, τ_3 = 6.6 μs, τ_4 = 100 μs, τ_5 = 400 μs, τ_6 = 20 μs.

The values of the branching ratios [10] are: β_{10} = 1.000, β_{21} = 0.387, β_{20} = 0.613, β_{32} = 0.999, β_{31} = 0.000, β_{30} = 0.001, β_{43} = 0.903, β_{42} = 0.006, β_{41} = 0.004, β_{40} = 0.087, β_{54} = 0.306, β_{53} = 0.012, β_{52} = 0.015, β_{51} = 0.179, β_{50} = 0.488, β_{65} = 0.941, β_{64} = 0.000, β_{63} = 0.002, β_{62} = 0.002, β_{61} = 0.004, β_{60} = 0.051.

Three ion-ion interactions are considered: ($^4S_{3/2}$+$^2H_{11/2}$, $^4I_{15/2}$) ↔ ($^4I_{9/2}$, $^4I_{13/2}$), ($^4I_{13/2}$, $^4I_{13/2}$) ↔ ($^4I_{15/2}$, $^4I_{9/2}$), and ($^4I_{11/2}$, $^4I_{11/2}$) ↔ ($^4I_{15/2}$, $^4F_{7/2}$), parameters are $W_{50} = 2\cdot10^{-23}m^3s^{-1}$, $W_{11} = 3\cdot10^{-23}m^3s^{-1}$ [2], and $W_{22} = 1.8\cdot10^{-23}m^3s^{-1}$ [2], respectively.

The Er^{3+} ions are pumped cw with P_{in} = 5 W at λ_p = 795 nm by ground-state absorption (GSA) $^4I_{15/2}\rightarrow{}^4I_{9/2}$ (cross-section $\sigma_{03} = 5\cdot10^{-21}cm^2$) and excited-state absorption (ESA) $^4I_{13/2}\rightarrow{}^2H_{11/2}$ ($\sigma_{15} = 1\cdot10^{-20}cm^2$). The laser transition is from the second Stark level of $^4I_{11/2}$ (Boltzmann population b_{22} = 0.200 at 300 K and degeneracy g_{22} = 2) into the fourth Stark level of $^4I_{13/2}$ (b_{14} = 0.113, g_{14} = 2) at λ_{Laser} = 2.81 µm with an emission cross-section $\sigma_{21} = 3\cdot10^{-20}cm^2$. The spontaneous radiative fraction on the laser transition is γ_{21} = 0.286.

The crystal has a length ℓ = 2 mm and a dopant concentration N = $2\cdot10^{21}cm^{-3}$. The resonator data are: optical length ℓ_{opt} = 0.1 m, incoupling efficiency of the pump light η = 0.56, average radius of the laser beam within the crystal r_{mode} = 250 µm, transmission of the outcoupling mirror Tr = 2 %. Only the fraction $P_1 / P = 10^{-7}$ of the spontaneous emission is emitted into the laser mode. c is the vacuum speed of light and h is the Planck constant.

The following rate equations for the population densities N_i and the photon density ϕ are solved for the 795 nm pump wavelength in a Runge-Kutta calculation:

$$dN_6/dt = -\tau_6^{-1} N_6 + W_{22} (N_2^2 - N_0 N_6)$$

$$dN_5/dt = R_{15} N_1 - \tau_5^{-1} N_5 + \beta_{65} \tau_6^{-1} N_6 - W_{50} (N_5 N_0 - N_3 N_1)$$

$$dN_4/dt = -\tau_4^{-1} N_4 + \Sigma_{i=5..6} (\beta_{i4} \tau_i^{-1} N_i)$$

$$dN_3/dt = R_{03} N_0 - \tau_3^{-1} N_3 + \Sigma_{i=4..6} (\beta_{i3} \tau_i^{-1} N_i) + W_{50} (N_5 N_0 - N_3 N_1) + W_{11} (N_1^2 - N_0 N_3)$$

$$dN_2/dt = -\tau_2^{-1} N_2 + \Sigma_{i=3..6} (\beta_{i2} \tau_i^{-1} N_i) - 2 W_{22} (N_2^2 - N_0 N_6) - R_{stE}$$

$$dN_1/dt = -R_{15} N_1 - \tau_1^{-1} N_1 + \Sigma_{i=2..6} (\beta_{i1} \tau_i^{-1} N_i) + W_{50} (N_5 N_0 - N_3 N_1) - 2 W_{11} (N_1^2 - N_0 N_3) + R_{stE}$$

$$dN_0/dt = -R_{03} N_0 + \Sigma_{i=1..6} (\beta_{i1} \tau_i^{-1} N_i) - W_{50} (N_5 N_0 - N_3 N_1) + W_{11} (N_1^2 - N_0 N_3) + W_{22} (N_2^2 - N_0 N_6)$$

$$d\phi/dt = (\ell / \ell_{opt}) [(P_1 / P) \gamma_{21} \beta_{21} \tau_2^{-1} N_2 + R_{stE}] + \ln(1-Tr)\, c\, \phi / 2 \ell_{opt}$$

$$R_{stE} = [b_{22} N_2 - (g_{22} / g_{14}) b_{14} N_1] \sigma_{21} c \phi$$

$$R_{ij} = [\sigma_{ij} / (\sigma_{03} N_0 + \sigma_{15} N_1)]\cdot [\lambda_p / (h c \ell \pi r_{mode}^2)]\cdot [1 - \exp\{-(\sigma_{03} N_0 + \sigma_{15} N_1) \ell\}] \eta P_{in}$$

The pump-rate terms R_{ij} are specific for the 795 nm pump wavelength.

The Influence of the Pump Level

Solving the rate equations for different pump wavelengths provides deeper insight into the population mechanisms of the Er^{3+}:$LiYF_4$ laser levels. The processes which are relevant for the cw operation of the Er^{3+} 3 µm laser are indicated in the level scheme of Fig. 1.

Pumping directly into the lower laser level at 1.53 µm leads to stimulated emission in both the simulation and experiments [3,4]. The calculation predicts that the slope efficiency is 18% with the threshold at 1.4 W. The excitation of the $^4I_{13/2}$ level is upconverted into the upper laser level via W_{11} and the subsequent multiphonon relaxation β_{32}.

The 970 nm pump wavelength into the $^4I_{11/2}$ upper laser level is the best choice for pumping the Er^{3+}:$LiYF_4$ crystal, in agreement with experiments [5]. The laser has a threshold of 0.5 W and a slope efficiency of 29 %.

Pumping at 795 nm into the $^4I_{9/2}$ level leads to 0.9 W threshold and a slope efficiency of 19 %. This wavelength exhibits two disadvantages: The multiphonon relaxation from the $^4I_{9/2}$ level reduces the quantum efficiency and results in the heating of the crystal and the higher population of the $^4I_{9/2}$ level enhances the inverse upconversion W_{11}^{-1} which populates the lower laser level and reduces stimulated emission.

The Kr^+ pump wavelength at 647 nm into the $^4F_{9/2}$ level suffers from the same negative aspects as the 795 nm wavelength, with additional losses being introduced by the multiphonon relaxation β_{43} and the ground-state fluorescence β_{40}.

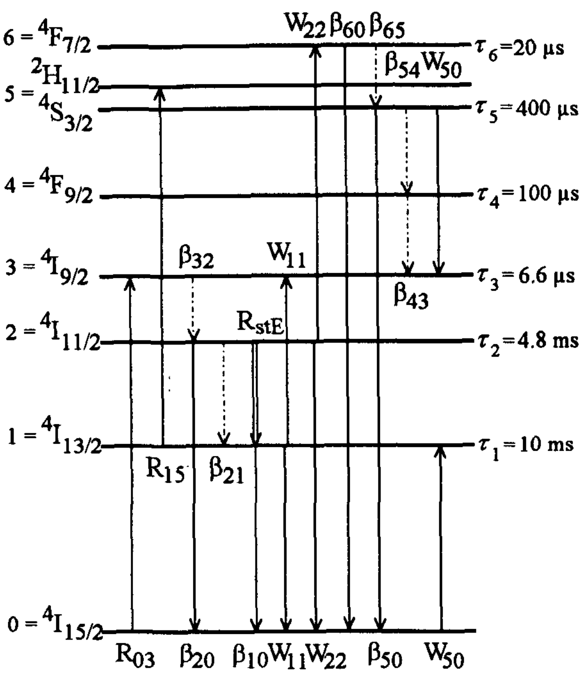

Figure 1. Er^{3+}:$LiYF_4$ level scheme indicating the processes which are relevant for the excitation of the laser levels. GSA (R_{03}) and ESA (R_{15}) are indicated only for the 795 nm pump wavelength.

The application of a green Kr^+ pump wavelength at 520 nm into the ${}^2H_{11/2}$ level leads to somewhat different population mechanisms. A threshold of 1.1 W and a slope efficiency of 20 % is calculated, which is comparable to the 795 nm pump wavelength. The pump excitation is efficiently down-converted to the ${}^4I_{9/2}$ level by the cross relaxation W_{50}, and via the multiphonon relaxation β_{32} to the upper laser level.

Pumping at 488 nm into the ${}^4F_{7/2}$ level leads to a threshold of 0.8 W and a slope efficiency of 23 %. After the multiphonon decay β_{65} the cross relaxation from the ${}^4S_{3/2}$ level avoids further multiphonon relaxations. The higher population of the ${}^4F_{7/2}$ level enhances the inverse upconversion W_{22}^{-1} and reduces the net sum upconverted from ${}^4I_{11/2}$ by $W_{22} - W_{22}^{-1}$.

Parameter Variations and Discussion

In three-dimensional parameter variations the dependence of several parameters on each other and their influence on output power is investigated. We assumed pumping cw at 795 nm with P_{in} = 5 W into the ${}^4I_{9/2}$ level. The varied parameters are the lifetimes of all levels, the upconversion parameters and the ESA cross section at 795 nm from the ${}^4I_{13/2}$ level.

Pump ESA at 795 nm on the transition ${}^4I_{13/2} \rightarrow {}^2H_{11/2}$ becomes relevant only at cross sections of above $1 \cdot 10^{-19} cm^2$, which are not present in crystals such as $LiYF_4$, YAG, or $YAlO_3$ [11]. The absence of this ESA does not significantly reduce laser output.

In a three level system the ratio of the populations of the upper (2) and lower (1) excited level is not simply determined by the ratio of the intrinsic lifetimes τ_i but is dependent on the feeding of level 1 through level 2 [7]. CW inversion is, therefore, obtained in $LiYF_4$ and BaY_2F_8 in the complete absence of upconversion processes. Er^{3+}:$LiYF_4$ has lifetimes τ_2 = 4.8 ms and τ_1 = 10 ms and a low branching ratio β_{21} = 0.387 from upper to lower laser level which leads to a ratio N_2 / N_1 = 1.24 of the multiplett-population densities. The ratio is even higher, if the Boltzmann populations of the lasing Stark sublevels are taken into account. Er^{3+}:BaY_2F_8 with τ_2 = 9.6 ms, τ_1 = 10.6 ms, and β_{21} = 0.35 [6] also exhibits cw inversion without upconversion. The situation in other crystals is different: higher phonon energies reduce the ${}^4I_{11/2}$ lifetime and draw the branching ratio β_{21} towards unity.

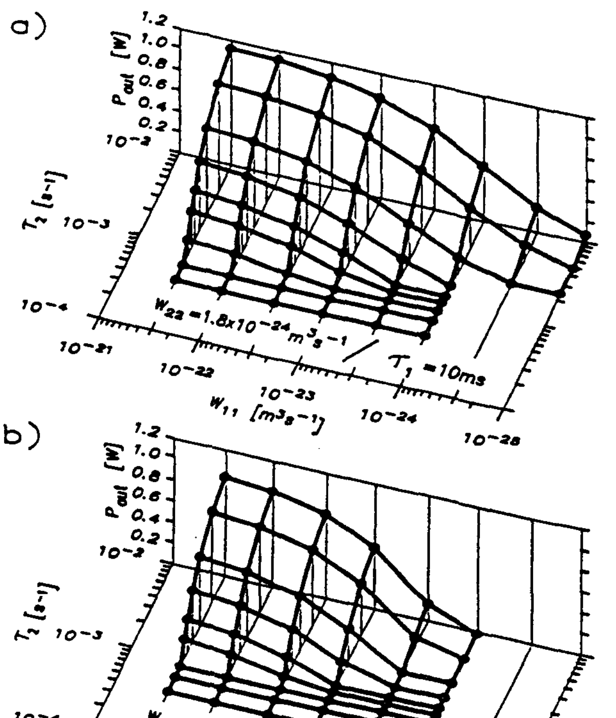

Figure 2. Variation P_{out} (τ_2, W_{11}, W_{22}): (a) W_{22} = $1.8 \cdot 10^{-24} m^3 s^{-1}$, (b) W_{22} = $1.8 \cdot 10^{-23} m^3 s^{-1}$. Explanations see text.

In the presence of upconversion the lifetime of the $^4I_{11/2}$ upper laser level still has a large influence on laser performance (Fig. 2). τ_2 should be as long as possible and in the Er^{3+}:$LiYF_4$ parameter configuration there is a lower limit for τ_2 of approximately 800 µs for cw operation (Fig. 2, left hand side). This limit increases to several ms when reducing W_{11}, because this reduces the depletion of the lower laser level (Fig. 2, right hand side). Er^{3+}:YAG suffers from high phonon energies. This results in a low lifetime τ_2 = 100 µs and a high branching ratio into the lower laser level due to multiphonon relaxation. The lower limit of τ_2 suppresses 3 µm cw lasing in Er^{3+}:YAG at 795 nm pumping.

The ratios of the inverse to the normal upconversion rates in Er^{3+}:$LiYF_4$ with the given pump conditions are W_{11}^{-1} / W_{11} = 0.54 and W_{22}^{-1} / W_{22} = 0.40. This demonstrates the necessity of considering the inverse upconversion processes W_{11}^{-1} and W_{22}^{-1} in the rate equations. The process W_{50}^{-1} is very weak.

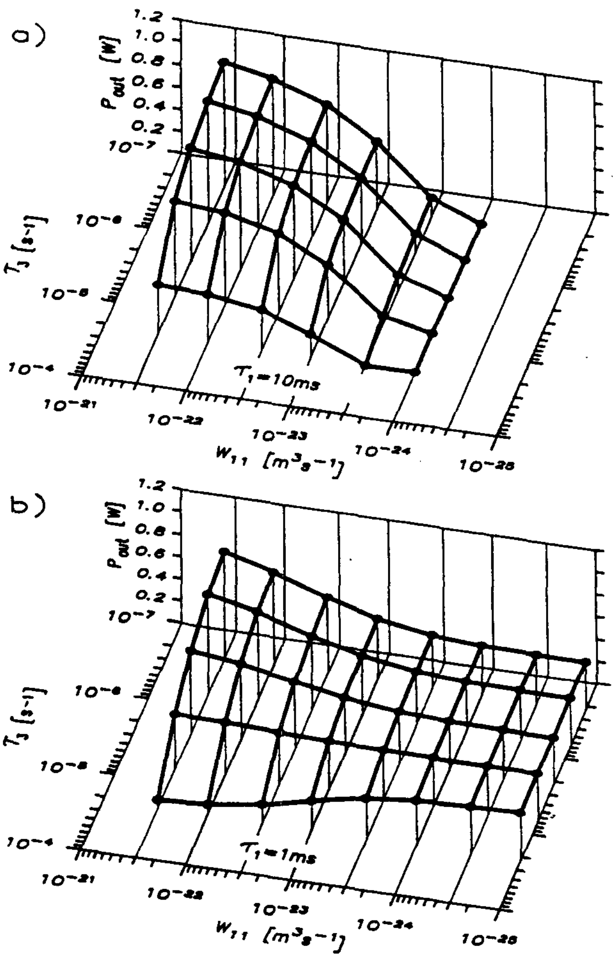

Figure 3. Variation P_{out} (τ_1, W_{11}, τ_3): (a) τ_1 = 10 ms, (b) τ_1 = 1 ms. Explanations see text.

The upconversion W_{11}, which is mainly responsible for efficient 3 µm lasing, is in competition with the inverse upconversion W_{11}^{-1} and the 1.6 µm fluorescence β_{10}. If the parameter W_{11} is large (Fig. 3, left hand side), the $^4I_{9/2}$ lifetime should be short to prevent W_{11}^{-1} from increasing (Figs. 3a and b). Decreasing τ_1 by co-doping decreases the population of the $^4I_{13/2}$ level, thus weakening the upconversion W_{11} and reducing the laser output (Fig. 3b).

If the parameter W_{11} is small (Fig. 3, right hand side), τ_3 has no influence on lasing because W_{11}^{-1} decreases with W_{11} (Figs. 3a and b). Maintaining a long τ_1, thus preventing any depletion of the $^4I_{13/2}$ level, terminates cw laser action because W_{22} is still active (Fig. 3a). The quenching of the $^4I_{13/2}$ lifetime by co-doping is now favorable (Fig. 3b). Promising co-dopants are Pr^{3+} [6] and Tb^{3+} [12]. There are combinations of the lifetimes τ_1 and τ_3, at which W_{11} and W_{11}^{-1} have the same rate and the laser performance becomes independent of the magnitude of the parameter W_{11}. When further reducing τ_1 or increasing τ_3 the W_{11}^{-1} process prevails over W_{11}, competing with β_{32}, populating the lower laser level and reducing the laser output (Fig. 3b, front).

The upconversion W_{22} is depleting the upper laser level, which reduces the laser output (Fig. 2b). The relation between τ_6 and W_{22} is the same as for τ_3 and W_{11}, but with the opposite effect on lasing: a long τ_6 maintains a larger population in $^4F_{7/2}$, which supports the cross relaxation W_{22}^{-1} and reduces the depletion of the $^4I_{11/2}$ level via the net sum W_{22} - W_{22}^{-1}.

The cross relaxation W_{50} is fed by the upconversion W_{22} and the subsequent multiphonon relaxation β_{65}. In the standard configuration the depopulation of the upper laser level via W_{22} is redistributed via W_{50} into the $^4I_{13/2}$ and $^4I_{9/2}$ levels, regardless of the value of W_{22}. An increase of W_{50} has no effect. Decreasing W_{50} leads to its saturation, whereas a decrease of the lifetime τ_5 introduces a relaxation channel, which is in competition with W_{50}. In both cases the upconverted energy is mostly lost directly to the ground state via W_{22} ($^4I_{11/2} \rightarrow {}^4I_{15/2}$) and to ground-state fluorescence (e.g. $^4S_{3/2} \rightarrow {}^4I_{15/2}$) as well as multiphonon relaxations ($^4S_{3/2} \rightarrow {}^4F_{9/2} \rightarrow {}^4I_{9/2}$). This leads to a decrease of the redistributed energy and a decrease of the laser output. The difference in output power for a small and a large W_{50} is more significant, if a larger part of the excitation leaves the upper laser level via W_{22} to be redistributed by W_{50}.

The benefit of co-doping with Cr^{3+} is present only in crystals with large W_{22} and small τ_5 like YSGG and YAG. In this case W_{50} cannot compensate for the depletion of the upper laser level via W_{22} and redistribute the lost energy. The energy transfer from the Er^{3+} $^4S_{3/2}$ level via Cr^{3+} into the Er^{3+} $^4I_{11/2}$ and $^4I_{9/2}$ levels takes over the role of W_{50}.

The Er^{3+}:$LiYF_4$ laser pumped with 5 W cw into the $^4I_{9/2}$ level has effective lifetimes $(1/\tau_2+W_{22}N_2)^{-1}$ = 1.4 ms in the $^4I_{11/2}$ level and $(1/\tau_1+W_{11}N_1)^{-1}$ = 0.89 ms in the $^4I_{13/2}$ level, and the 3 μm laser is not self-terminating in this case. Since the populations of the laser levels also depend on the energy-feeding mechanisms of the laser levels, the ratio of the intrinsic lifetimes of $^4I_{11/2}$ and $^4I_{13/2}$ has been misunderstood as an indication for the possibility of cw lasing.

Conclusions

We have developed a program for the full simulation of the Erbium laser including all relevant processes and a realistic resonator design. The evaluation shows that, in the frame of the available parameters, the fluorides $LiYF_4$ and BaY_2F_8 are currently the best choice as host materials for the Er^{3+} 3 μm laser.

The 970 nm pump wavelength has two advantages in comparison to 795 nm pumping: It avoids the multiphonon relaxation from the $^4I_{9/2}$ level, thus increasing the quantum efficiency, and the lower population of the $^4I_{9/2}$ level reduces the inverse upconversion from the $^4I_{9/2}$ level into the lower laser level.

CW inversion can be obtained in the absence of upconversion processes because of a long lifetime of the upper laser level and a favorable low branching ratio into the lower laser level.

The strong upconversion from the $^4I_{13/2}$ level has a major effect on stimulated emission by efficiently depleting the lower and feeding the upper laser level. In the presence of upconversion the lifetime of the lower laser level should be as long as possible. The quenching of this level by co-doping decreases the upconversion W_{11} without simultaneously decreasing the inverse process W_{11}^{-1} and thus reduces the output power of the laser. Upconversion from the upper laser level is detrimental to stimulated emission but may be compensated by cross relaxation from the $^4S_{3/2}$ level.

The lifetime of the upper laser level must be longer than 800 μs for cw-laser operation. Despite the influence of upconversion this lifetime is the most crucial parameter for the efficient cw-laser operation of the Er^{3+} 3 μm laser.

Acknowledgements

We thank H.J. Weder for his help with the figures. This work was supported in part by the Swiss Priority Program "Optique".

References

[1] K. S. Bagdasarov, V. I. Zhekov, V. A. Lobachev, T. M. Murina, and A. M. Prokhorov, "Steady-state stimulated emission from $Y_3Al_5O_{12}$:Er^{3+} laser (λ = 2.94 μm, T = 300 K)", Kvant. Elektr.10, 452 (1983).

[2] H. Chou and H. P. Jenssen, "Upconversion processes in Er-activated solid state materials", in Tunable Solid State Lasers, Vol. 5 of the OSA Proceeding Series, M. L. Shand and H. P. Jenssen, eds. (Opt. Soc. Am., Washington, D.C., 1989), pp. 167-174.

[3] P. Xie and S. C. Rand, "Continuous wave, pair-pumped laser", Opt. Lett. 15(15), 848-850 (1990).

[4] S. A. Pollack, D. B. Chang, M. Birnbaum, and M. Kokta, "Upconversion-pumped 2.8-2.9 μm lasing of Er^{3+} ion in garnets", J. Appl. Phys. 70(12), 7227 (1991).

[5] R. C. Stoneman, J. G. Lynn, and L. Esterowitz, "Direct upper-state pumping of 2.8 μm Er^{3+}:YLF Laser", IEEE J. Quantum Electron. 28(4), 1041 (1992).

[6] D. S. Knowles and H. P. Jenssen, "Upconversion versus Pr-deactivation for Efficient 3 μm Laser Operation in Er", IEEE J. Quantum Electron. 28(4), 1197-1208 (1992).

[7] R. S. Quimby and W. J. Miniscalco, "Continuous-wave lasing on a self-terminating transition", Appl. Opt. 28(1), 14 (1989).

[8] W. Lüthy and H.P. Weber, "The 3 μm erbium laser", Infrared Phys. 32, 283 (1991).

[9] V. Lupei, S. Georgescu, and V. Florea, "On the dynamics of population inversion for 3 μm Er^{3+} lasers", IEEE J. Quantum Electron. 29(2), 426 (1993).

[10] C. Li, Y. Guyot, C. Linarès, R. Moncorgé, and M. F. Joubert, "Radiative transition probabilities of trivalent rare-earth ions in $LiYF_4$", in Advanced Solid-State Lasers and Compact Blue-Green Lasers Technical Digest, 1993 (Optical Society of America, Washington, D.C., 1993), Vol.2, pp.423-425.

[11] M. Pollnau, E. Heumann, and G. Huber, "Time-resolved spectra of excited-state absorption in Er^{3+} doped $YAlO_3$", Appl. Phys. A 54(5), 404 (1992).

[12] M. Pollnau, E. Heumann, and G. Huber, "Stimulated emission and excited-state absorption at room temperature on the 550 nm-laser transition in Er^{3+} doped $YAlO_3$", to appear in J. Lumin. (1994).